Available online at www.sciencedirect.com
ScienceDirect
International Journal of Thermal Sciences 47 (2008) 1276–1283
International Journal of Thermal Sciences
www.elsevier.com/locate/ijts

Modelling of thermal contact resistance within the framework of the thermal lattice Boltzmann method

K. Han *, Y.T. Feng, D.R.J. Owen

Civil and Computational Engineering Centre, School of Engineering, Swansea University, SA2 8PP, UK

Received 27 July 2007; received in revised form 24 November 2007; accepted 26 November 2007

Available online 3 January 2008

Abstract

A novel numerical approach, termed the partial bounce back scheme, is introduced within the framework of the thermal lattice Boltzmann method to account for thermal contact resistance between contacting surfaces. The correlation between thermal contact resistance and the partial bounce back parameter is established. A special case of the scheme leads to a new approach that can be directly applied for the treatment of adiabatic thermal boundary conditions in the thermal lattice Boltzmann method. Numerical examples are provided to validate and demonstrate the accuracy and effectiveness of the proposed methodology.

Keywords: Heat transfer; Thermal contact resistance; Thermal lattice Boltzmann method; Partial bounce back scheme

1. Introduction

In recent years, the lattice Boltzmann method (LBM) has emerged as an alternative to conventional computational fluid dynamics methods employing Navier–Stokes equations. It has found extensive applications in simulating isothermal flows of various complexities, see for instance [1–8]. There has also been an ongoing effort in the construction of stable thermal lattice Boltzmann methods (TLBM) to solve heat transfer problems. In the early works, the isothermal lattice Boltzmann model is extended with additional velocities to obtain the temperature evolution. The inclusion of higher order velocity terms in the LBM leads to numerical instabilities and hence the temperature variation is limited to a narrow range. To overcome the defects, He et al. [9] introduce a double population approach, using a density distribution function to simulate hydrodynamics for fluid flows and an internal energy distribution function to simulate thermodynamics for heat transfer. This model has better numerical stability and the viscous heat dissipation and compression work done by the pressure can be solved fundamentally. As a result, it has been extensively adopted by researchers to solve various thermo-hydrodynamic problems [10–13].

With regard to the thermal boundary conditions, several methods have been developed. D'Orazio et al. [14] propose a thermal counter-slip approach, in which a counter-slip thermal energy density is assumed for boundary nodes and is determined consistently with Dirichlet or Neumann boundary constraints; Tang et al. [15] introduce a thermal boundary treatment by decomposing the internal energy distribution functions at the boundary nodes into equilibrium and nonequilibrium parts; Huang et al. [16] propose a thermal curved wall boundary scheme based on the idea of non-slip wall boundary treatment for isothermal LBM.

In this work, we attempt to incorporate thermal contact resistance into the thermal lattice Boltzmann framework. Thermal contact resistance exists when two solid bodies come in contact. Heat flows from the hotter body to the colder body, and a temperature drop is usually observed at the interface between the two surfaces in contact. Thermal contact resistance can be very important in a number of applications. It is however a complicated phenomenon influenced by many factors, among which surface roughness is believed to play a central role as no real surface is perfectly smooth. Unfortunately there is no satisfactory theory which will predict thermal contact resistance for all

* Corresponding author.
E-mail address: k.han@swansea.ac.uk (K. Han).

1290-0729/$ – see front matter
doi:10.1016/j.ijthermalsci.2007.11.007

Nomenclature

$f_i, \bar{f}_i$	fluid density distribution function in the ith direction	p	pressure
f_i^{eq}	fluid equilibrium distribution function in the ith direction	T	temperature
$g_i, \bar{g}_i$	internal energy distribution functions in the ith direction	q	heat flux
g_i^{eq}	internal energy equilibrium distribution function in the ith direction	ρ	fluid density
$\mathbf{e}_i$	discrete velocity in the ith direction	ϵ	internal energy per unit mass
Z_i	effect of viscous heating	c	lattice speed
t	time	c_s	fluid speed of sound
Δt	time step	μ	kinematic viscosity
τ_f	non-dimensional fluid relaxation time	α	thermal diffusivity
τ_g	non-dimensional internal energy relaxation time	κ_g	thermal conductivity
$\mathbf{u}$	velocity vector	δ	partial bounce back parameter
		R_g, R_T	thermal resistance per lattice, total thermal resistance
		R_c	thermal contact resistance

types of engineering materials, nor have experimental studies yielded completely reliable empirical correlations [17].

A novel numerical approach, termed the *partial bounce back* (*PBB*) scheme, is proposed within the TLBM framework to account for the effect of thermal contact resistance between the contacting surfaces. The PPB scheme can also be applied for the treatment of adiabatic thermal boundary conditions in a straight forward manner.

2. The thermal lattice Boltzmann method

In the double population thermal lattice Boltzmann method (TLBM) proposed by He et al. [9], the flow and the temperature fields are solved by the following two evolution equations

$$\bar{f}_i(\mathbf{x}+\mathbf{e}_i\Delta t, t+\Delta t) - \bar{f}_i(\mathbf{x},t) = -\frac{1}{\tau_f+0.5}\left[\bar{f}_i(\mathbf{x},t) - f_i^{\mathrm{eq}}(\mathbf{x},t)\right] \tag{1}$$

$$\bar{g}_i(\mathbf{x}+\mathbf{e}_i\Delta t, t+\Delta t) - \bar{g}_i(\mathbf{x},t) = -\frac{1}{\tau_g+0.5}\left[\bar{g}_i(\mathbf{x},t) - g_i^{\mathrm{eq}}(\mathbf{x},t)\right] - \frac{\tau_g}{\tau_g+0.5} f_i Z_i \tag{2}$$

where

$$\bar{f}_i = f_i + \frac{0.5}{\tau_f}\left(f_i - f_i^{\mathrm{eq}}\right) \tag{3}$$

$$\bar{g}_i = g_i + \frac{0.5}{\tau_g}\left(g_i - g_i^{\mathrm{eq}}\right) + \frac{\Delta t}{2} f_i Z_i \tag{4}$$

in which f_i and g_i are respectively the density distribution function and the internal energy distribution function with discrete velocity $\mathbf{e}_i$ along the ith direction; f_i^{eq} and g_i^{eq} are the corresponding equilibrium distribution functions; τ_f and τ_g are respectively the *non-dimensional* momentum and internal energy relaxation times which control the rate of change to equilibrium; and Δt is the time step. The left-hand sides of Eqs. (1) and (2) denote the streaming process while the right-hand sides model the collisions through relaxation.

The term $Z_i = (\mathbf{e}_i - \mathbf{u}) \cdot [\partial\mathbf{u}/\partial t + (\mathbf{e}_i \cdot \nabla)\mathbf{u}]$ represents the effect of viscous heating and can be expressed as [14]

$$Z_i = \frac{(\mathbf{e}_i - \mathbf{u}) \cdot [\mathbf{u}(\mathbf{x}+\mathbf{e}_i\Delta t, t+\Delta t) - \mathbf{u}(\mathbf{x},t)]}{\Delta t} \tag{5}$$

In the widely used D2Q9 model, the fluid particles at each node move to their eight immediate neighbouring nodes with discrete velocities $\mathbf{e}_i$ $(i = 1, \ldots, 8)$. A proportion of the particles can remain at the node, which is equivalent to moving with a zero velocity $\mathbf{e}_0$. The nine discrete velocity vectors are given by

$$\begin{cases} \mathbf{e}_0 = (0,0) \\ \mathbf{e}_1 = c(1,0); \quad \mathbf{e}_2 = c(0,1) \\ \mathbf{e}_3 = c(-1,0); \quad \mathbf{e}_4 = c(0,-1) \\ \mathbf{e}_5 = c(1,1); \quad \mathbf{e}_6 = c(-1,1) \\ \mathbf{e}_7 = c(-1,-1); \quad \mathbf{e}_8 = c(1,-1) \end{cases} \tag{6}$$

where $c = \Delta x/\Delta t$ is the lattice speed with Δx being the lattice spacing. For gas flows, c can be defined as

$$c = \sqrt{3RT_m}$$

where R is the gas constant and T_m the average temperature.

The equilibrium distribution functions f_i^{eq} and g_i^{eq} are defined in the D2Q9 model respectively as

$$f_i^{\mathrm{eq}} = w_i\rho\left[1 + \frac{3(\mathbf{e}_i\cdot\mathbf{u})}{c^2} + \frac{9(\mathbf{e}_i\cdot\mathbf{u})^2}{2c^4} - \frac{3(\mathbf{u}\cdot\mathbf{u})}{2c^2}\right] \tag{7}$$

and

$$\begin{cases} g_0^{\mathrm{eq}} = w_0\rho\epsilon\left[-\dfrac{3(\mathbf{u}\cdot\mathbf{u})}{2c^2}\right] \\ g_i^{\mathrm{eq}} = w_i\rho\epsilon\left[\dfrac{3}{2} + \dfrac{3(\mathbf{e}_i\cdot\mathbf{u})}{2c^2} + \dfrac{9(\mathbf{e}_i\cdot\mathbf{u})^2}{2c^4} - \dfrac{3(\mathbf{u}\cdot\mathbf{u})}{2c^2}\right] \\ \qquad (i = 1,2,3,4) \\ g_i^{\mathrm{eq}} = w_i\rho\epsilon\left[3 + \dfrac{6(\mathbf{e}_i\cdot\mathbf{u})}{c^2} + \dfrac{9(\mathbf{e}_i\cdot\mathbf{u})^2}{2c^4} - \dfrac{3(\mathbf{u}\cdot\mathbf{u})}{2c^2}\right] \\ \qquad (i = 5,6,7,8) \end{cases} \tag{8}$$

in which w_i are the weighting factors with $w_0 = 4/9$, $w_i = 1/9$ for $i = 1,2,3,4$ and $w_i = 1/36$ for $i = 5,6,7,8$; and $\rho\epsilon$ is

the internal energy which can be replaced by temperature T to simplify the calculation of g_i if the flow is incompressible or the compressibility can be ignored.

The macroscopic variables, such as density ρ, velocity $\mathbf{u}$, internal energy per unit mass ϵ, and heat flux q, can be calculated from the zeroth and first order moments of the distribution functions as

$$\rho = \sum \bar{f}_i; \quad \rho\mathbf{u} = \sum \bar{f}_i \mathbf{e}_i$$
$$\rho\epsilon = \sum \bar{g}_i - \frac{\Delta t}{2}\sum f_i Z_i$$
$$\mathbf{q} = \left(\sum \mathbf{e}_i \bar{g}_i - \rho\epsilon\mathbf{u} - \frac{\Delta t}{2}\sum \mathbf{e}_i f_i Z_i\right)\frac{\tau_g}{\tau_g + 0.5} \tag{9}$$

The fluid pressure p is determined by the equation of state

$$p = c_s^2 \rho \tag{10}$$

where c_s is termed the fluid speed of sound and is related to the lattice speed c by

$$c_s = c/\sqrt{3} \tag{11}$$

The kinematic viscosity ν and thermal diffusivity α of the fluid are determined as

$$\nu = \frac{1}{3}\tau_f c^2 \Delta t; \qquad \alpha = \frac{2}{3}\tau_g c^2 \Delta t \tag{12}$$

Note that for solids, the above equations are much simpler due to $\mathbf{u} = 0$.

3. Modelling of thermal contact resistance within the framework of TLBM

3.1. Derivation of thermal resistance in TLBM

Consider a steady-state heat conduction problem in a 2D rectangular bar, as shown in Fig. 1. Both the top and bottom sides of the bar are insulated. Heat flows only in the axial direction, and thus it is equivalent to a 1D heat conduction problem. Assume that nodes I and J are two adjacent nodes in the lattice discretisation of the bar. Under steady state conditions, the following relations can be established for some internal energy distribution functions:

$$g_2 = g_4 = g_2^{\mathrm{eq}} = \frac{1}{6}T; \qquad g_5 = g_8; \qquad g_6 = g_7 \tag{13}$$

The axial heat flux at each node is calculated as

$$q_x = \left(\sum e_{i,x} g_i\right)\frac{\tau_g}{\tau_g + 0.5} \tag{14}$$

where $e_{i,x}$ is the x component of $\mathbf{e}_i$.

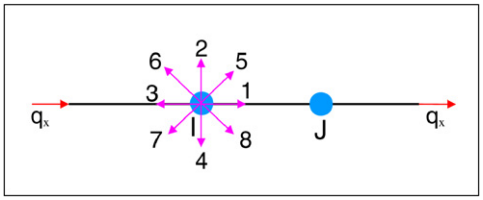

Fig. 1. Heat conduction in a 2D uniform bar with the top and bottom sides insulated.

Denoting $q'_x = \sum e_{i,x} g_i$, we have

$$q'_x = g_1^I - g_3^I + 2\left(g_5^I - g_7^I\right)$$
$$= g_1^J - g_3^J + 2\left(g_5^J - g_7^J\right) \tag{15}$$

The temperature at node I is given by

$$T^I = \sum g_i^I$$

By making use of the relations in Eq. (13), the above equation can be rewritten as

$$\frac{2}{3}T^I = g_1^I + g_3^I + 2\left(g_5^I + g_7^I\right) \tag{16}$$

Combining Eqs. (15) and (16) gives

$$\begin{cases} g_1^I + 2g_5^I = \dfrac{1}{3}T^I + \dfrac{1}{2}q'_x \\ g_3^I + 2g_7^I = \dfrac{1}{3}T^I - \dfrac{1}{2}q'_x \end{cases} \tag{17}$$

Similarly, the following relations hold for node J:

$$\begin{cases} g_1^J + 2g_5^J = \dfrac{1}{3}T^J + \dfrac{1}{2}q'_x \\ g_3^J + 2g_7^J = \dfrac{1}{3}T^J - \dfrac{1}{2}q'_x \end{cases} \tag{18}$$

According to the evolution equation of the internal energy distribution functions, g_1^J and g_5^J are calculated as

$$\begin{cases} g_1^J = g_1^I - \dfrac{1}{\tau_g + 0.5}\left(g_1^I - \dfrac{1}{6}T^I\right) \\ g_5^J = g_5^I - \dfrac{1}{\tau_g + 0.5}\left(g_5^I - \dfrac{1}{12}T^I\right) \end{cases} \tag{19}$$

By substituting Eq. (19) into Eqs. (17) and (18), q'_x can be expressed as

$$q'_x = \Delta T \Big/ \frac{3}{2(\tau_g + 0.5)}$$

where $\Delta T = T^I - T^J$ denotes the temperature difference between nodes I and J. Then the heat flux per lattice grid is determined as

$$q_x = \frac{\tau_g}{\tau_g + 0.5} q'_x = \Delta T \Big/ \frac{3}{2\tau_g} \tag{20}$$

Thus the thermal resistance per lattice grid, R_g, is found to be

$$R_g = \frac{\Delta T}{q_x} = \frac{3}{2\tau_g} = \frac{c^2 \Delta t}{\alpha} \tag{21}$$

and the equivalent thermal conductivity is calculated as

$$\kappa_g = \frac{1}{R_g} = \frac{2\tau_g}{3} = \frac{\alpha}{c^2 \Delta t} \tag{22}$$

3.2. Partial bounce back scheme

Assume that Ω_1 and Ω_2 are two solid bodies in contact; I and J are two adjacent boundary nodes, respectively for Ω_1 and Ω_2, and the contact surface with a thermal contact resistance R_c lies in the middle of the link between nodes I and J, as

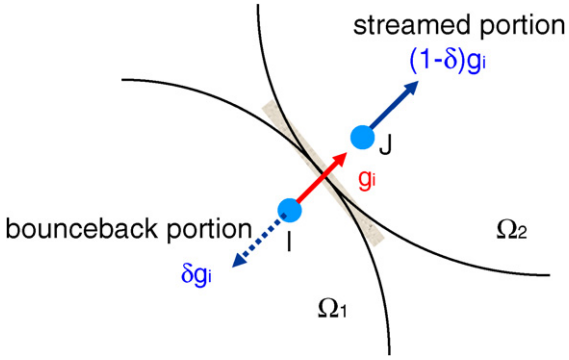

Fig. 2. Partial bounce back scheme: streamed density function in any direction is partially bounced back along the opposite direction.

indicated in Fig. 2. A *partial bounce back* (*PBB*) scheme within the TLBM framework is proposed in this work to account for thermal contact resistance.

The idea of the PBB scheme is simple: only a portion of the internal energy of a boundary node of body Ω_1/Ω_2 is allowed to propagate to its adjacent boundary node of body Ω_2/Ω_1, and the remaining portion is bounced back to the node itself with opposite direction. For instance, if g_i^I is the internal energy distribution function of boundary node I of body Ω_1 in the ith direction, and let δ denote a parameter between $[0, 1]$, then $(1-\delta)g_i^I$ is the amount to be streamed to node J, a boundary node of body Ω_2 adjacent to node I, while the amount δg_i^I is bounced back to node I in the direction $-i$.

It is important to choose the parameter δ so that the thermal contact resistance can be correctly represented. The following derivation aims to establish a correlation between δ and thermal contact resistance R_c. Referring to Fig. 2, the internal energy distribution functions of node I are obtained using the PPB scheme as

$$g_3^I = \delta\tilde{g}_1^I + (1-\delta)\tilde{g}_3^J \tag{23}$$

$$g_7^I = \delta\tilde{g}_5^I + (1-\delta)\tilde{g}_7^J \tag{24}$$

where

$$\tilde{g}_1^I = g_1^I - \frac{1}{\tau_g'}\left(g_1^I - \frac{1}{6}T^I\right) \tag{25}$$

$$\tilde{g}_5^I = g_5^I - \frac{1}{\tau_g'}\left(g_5^I - \frac{1}{12}T^I\right) \tag{26}$$

are the post-collision internal energy distribution functions and $\tau_g' = \tau_g + 0.5$. Combining Eqs. (25) and (26) gives

$$\tilde{g}_1^I + 2\tilde{g}_5^I = \left(1 - \frac{1}{\tau_g'}\right)\left(g_1^I + 2g_5^I\right) + \frac{1}{3\tau_g'}T^I \tag{27}$$

Similarly,

$$\tilde{g}_3^J = g_3^J - \frac{1}{\tau_g'}\left(g_3^J - \frac{1}{6}T^J\right) \tag{28}$$

$$\tilde{g}_7^J = g_7^J - \frac{1}{\tau_g'}\left(g_7^J - \frac{1}{12}T^J\right) \tag{29}$$

and

$$\tilde{g}_3^J + 2\tilde{g}_7^J = \left(1 - \frac{1}{\tau_g'}\right)\left(g_3^J + 2g_7^J\right) + \frac{1}{3\tau_g'}T^J \tag{30}$$

By summing Eqs. (23) and (24) and utilising Eq. (18), we have

$$\begin{aligned} g_3^I + 2g_7^I &= \delta\left(\tilde{g}_1^I + 2\tilde{g}_5^I\right) + (1-\delta)\left(\tilde{g}_3^J + 2\tilde{g}_7^J\right) \\ &= \frac{1}{3}T^I - \frac{1}{2}q_x' \end{aligned} \tag{31}$$

Substituting Eqs. (27) and (30) into the above equation and rearranging leads to the following expression for q_x'

$$q_x' = \frac{T^I - T^J}{R'}$$

where

$$R' = \frac{3}{1-\delta}\left(\delta - \frac{\delta}{\tau_g'} + \frac{1}{2\tau_g'}\right) \tag{32}$$

The heat flux equals

$$q_x = \frac{\tau_g}{\tau_g + 0.5}q_x' = \frac{2\tau_g' - 1}{2\tau_g'}q_x'$$

Consequently, the total thermal resistance R_T, including thermal contact resistance R_c, between nodes I and J is obtained as

$$R_T = \frac{2\tau_g'}{2\tau_g' - 1}R' = \frac{3\delta}{1-\delta} + \frac{3}{2\tau_g} \tag{33}$$

Since the lattice gird resistance $R_g = 3/2\tau_g$, the thermal contact resistance R_c of the two contacting bodies Ω_1 and Ω_2 is thus given by

$$R_c = R_T - R_g = \frac{3\delta}{1-\delta} \tag{34}$$

The corresponding equivalent thermal conductivity can be expressed as

$$\kappa_c = \frac{1}{R_c} = \frac{1-\delta}{3\delta} \tag{35}$$

Eqs. (34) and (35) provide the relationship between the partial bounce back parameter δ and the thermal contact resistance R_c or conductivity κ_c. With δ varying in $[0, 1]$, the effect of different thermal contact resistance can be achieved. In particular, when $\delta = 0$ no thermal contact resistance exists; whereas when $\delta = 1$, the incoming internal energy population is fully reflected back so that the contact surface serves as an insulated wall, which provides a new treatment for enforcing the fully insulated thermal boundary condition in the TLBM.

4. Numerical illustrations

4.1. Validation of the PPB scheme

To validate the proposed partial bounce back scheme, particularly the correlation in Eq. (34) between thermal contact resistance R_c and the parameter δ, a numerical example is provided.

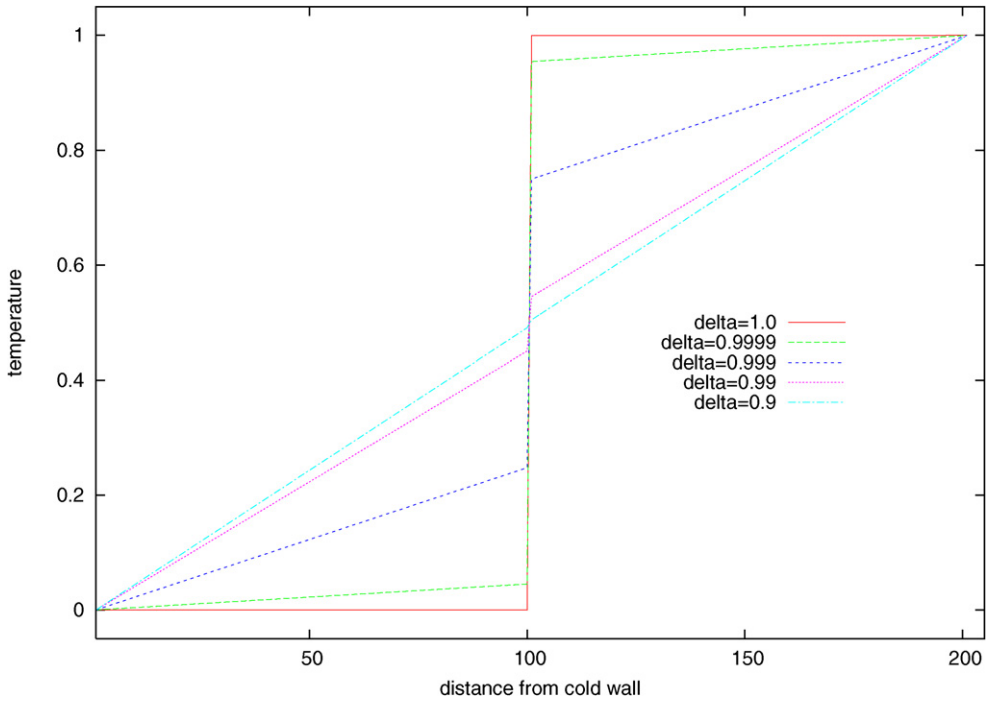

Fig. 3. Computed temperature distribution along the centerline of a 2D bar for different δ.

Table 1
Simulated and theoretical temperature drop at the contact surface

δ	0.5	0.8	0.9	0.99	0.999	0.9999	1.0
Theoretical	0.000505	0.00398	0.00892	0.09008	0.49975	0.90908	1.0
Simulated	0.000504	0.00396	0.00891	0.08996	0.49961	0.90896	0.99998

The problem considers two connected equally sized rectangular bars with thermal contact resistance at the interface. The bars have the same initial temperature (0°) and thermal properties. The left and right walls are maintained at different constant temperatures with $T_{\text{left}} = 0°$ and $T_{\text{right}} = 1°$, whereas the top and bottom walls are adiabatic to ensure a one-dimensional heat conduction situation. The domain is divided into a 200×20 lattice grid, and $\tau_g = 0.1$.

Simulated with the PPB scheme for different δ, the temperature distribution along the centerline of the bars is shown in Fig. 3. The temperature drop at the contact surface is very small for $\delta < 0.9$, then increases with the increase of δ. When $\delta = 1.0$, the contact surface becomes an insulated wall, i.e. no heat flows in or out of the surface. Table 1 gives a comparison of the temperature drop at the contact surface simulated with the PPB scheme and the theoretical value determined by

$$\Delta T_c = \frac{R_c}{R_c + nR_g} \tag{36}$$

where $n = 200$ is the number of lattice nodes in the axial direction of the bars. The derivation of this formula is trivial and thus omitted here. It is evident that an excellent agreement of the results is achieved and thus the relationship between δ and R_c given by (34) is validated.

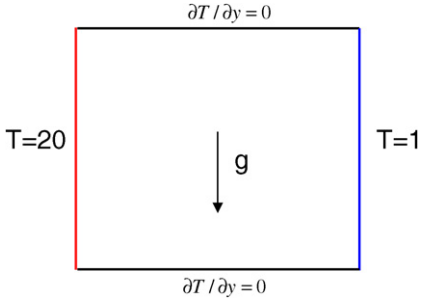

Fig. 4. Problem setup for natural convection in a square cavity.

4.2. Application of the PPB scheme to adiabatic thermal boundary conditions

The proposed partial bounce back scheme can also be directly applied to the treatment of adiabatic thermal boundary conditions in the TLBM when $\delta = 1$. Two problems are investigated to demonstrate its applicability.

The first example is based on D'Orazio's work [14] for simulating natural convection in a square cavity. The temperature difference between the left and right walls introduces a temperature gradient in the fluid, and the consequent density difference induces convection in the cavity. The top and bottom walls are adiabatic, as depicted in Fig. 4. With the Boussinesq approximation, all the fluid properties are considered as constant,

except the buoyancy term, which is assumed to depend linearly on the temperature, $\rho G = \rho\beta g(T - T_m)\mathbf{j}$, where β is the thermal expansion coefficient, g is the acceleration due to gravity, and $\mathbf{j}$ is the direction opposite to that of gravity. To account for the buoyancy effect, a force term is included in the evolution equation (1) of the fluid distribution functions as

$$\bar{f}_i(\mathbf{x}+\mathbf{e}_i\Delta t, t+\Delta t) - \bar{f}_i(\mathbf{x},t) = -\frac{1}{\tau_f + 0.5}\left[\bar{f}_i(\mathbf{x},t) - f_i^{\mathrm{eq}}(\mathbf{x},t)\right] + \frac{\tau_f}{\tau_f + 0.5}F_i$$

where

$$F_i = \frac{G(\mathbf{e}_i - \mathbf{u})}{RT} f_i^{\mathrm{eq}}$$

The major control parameter is the Rayleigh number $Ra = \beta g \Delta T H^3 Pr/\nu^2$, where ΔT is the temperature difference between the hot and cold walls; $Pr = \nu/\alpha$ is the Prandtl number, measuring the momentum to heat diffusivity ratio; and H is the height or width of the cavity. The diffusion velocity $U^* = \nu/(Pr\,H)$ is used to normalise the calculated velocities. In [14], D'Orazio et al. assume a counter-slip thermal energy density to handle Dirichlet and Neumann boundary conditions, which is consistent with the second-order accurate boundary treatment for fluid flow. We adopt their approach for the Dirichlet boundary treatment, but apply the PPB scheme with $\delta = 1$ for the adiabatic top and bottom walls. The simulations are performed for Rayleigh numbers ranging from 10^3 to 10^6, Prandtl number $Pr = 0.71$, and the relaxation times are chosen to be $\tau_f = 0.1$ and $\tau_g = 0.0704$. The lattice grid used is 129×129 for $Ra = 10^3$ and $Ra = 10^4$, and 205×205 for $Ra = 10^5$ and $Ra = 10^6$. The steady state temperature distribution is compared. Table 2 lists the normalised maximum horizontal veloc-

Table 2
Comparison of velocity solutions

	Rayleigh number	$u_{\max}(y/L)$	$v_{\max}(x/L)$
This work	$Ra = 10^3$	3.6520 (0.8125)	3.6960 (0.1797)
D'Orazio		3.6532 (0.8125)	3.7006 (0.1797)
This work	$Ra = 10^4$	16.2318 (0.8203)	19.6280 (0.1172)
D'Orazio		16.2370 (0.8203)	19.6803 (0.1172)
This work	$Ra = 10^5$	34.8905 (0.8578)	68.3229 (0.0637)
D'Orazio		34.8225 (0.8529)	68.7122 (0.0637)
This work	$Ra = 10^6$	64.4220 (0.8526)	218.9540 (0.0380)
D'Orazio		64.8679 (0.8529)	221.1869 (0.0392)

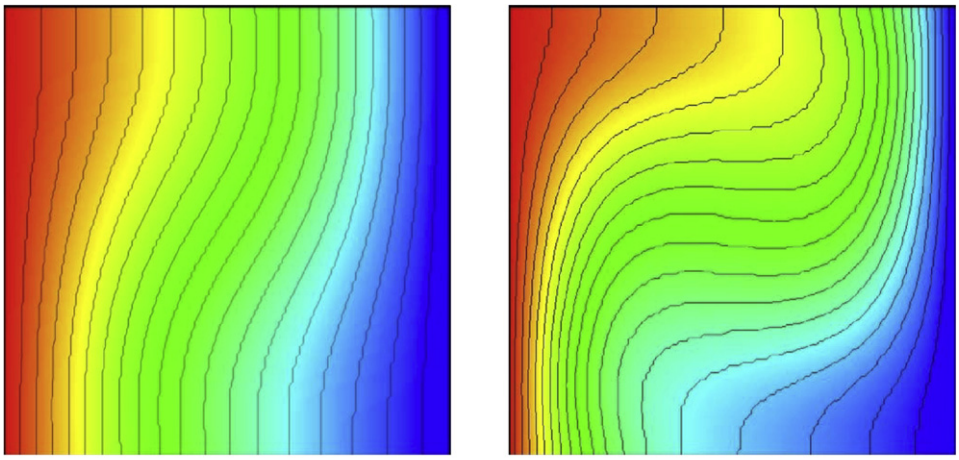

(a) $Ra = 10^3$ (b) $Ra = 10^4$

(c) $Ra = 10^5$ (d) $Ra = 10^6$

Fig. 5. Isothermal contours of natural convection in a square cavity for four different Rayleigh numbers.

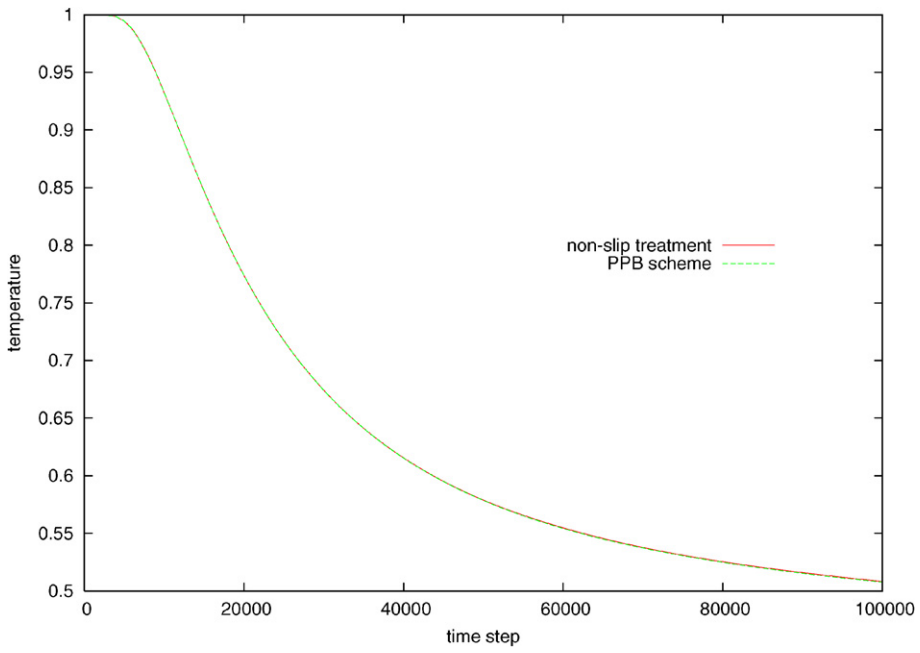

Fig. 6. Temperature history of particle No. 9 obtained by Huang's scheme and the PPB scheme.

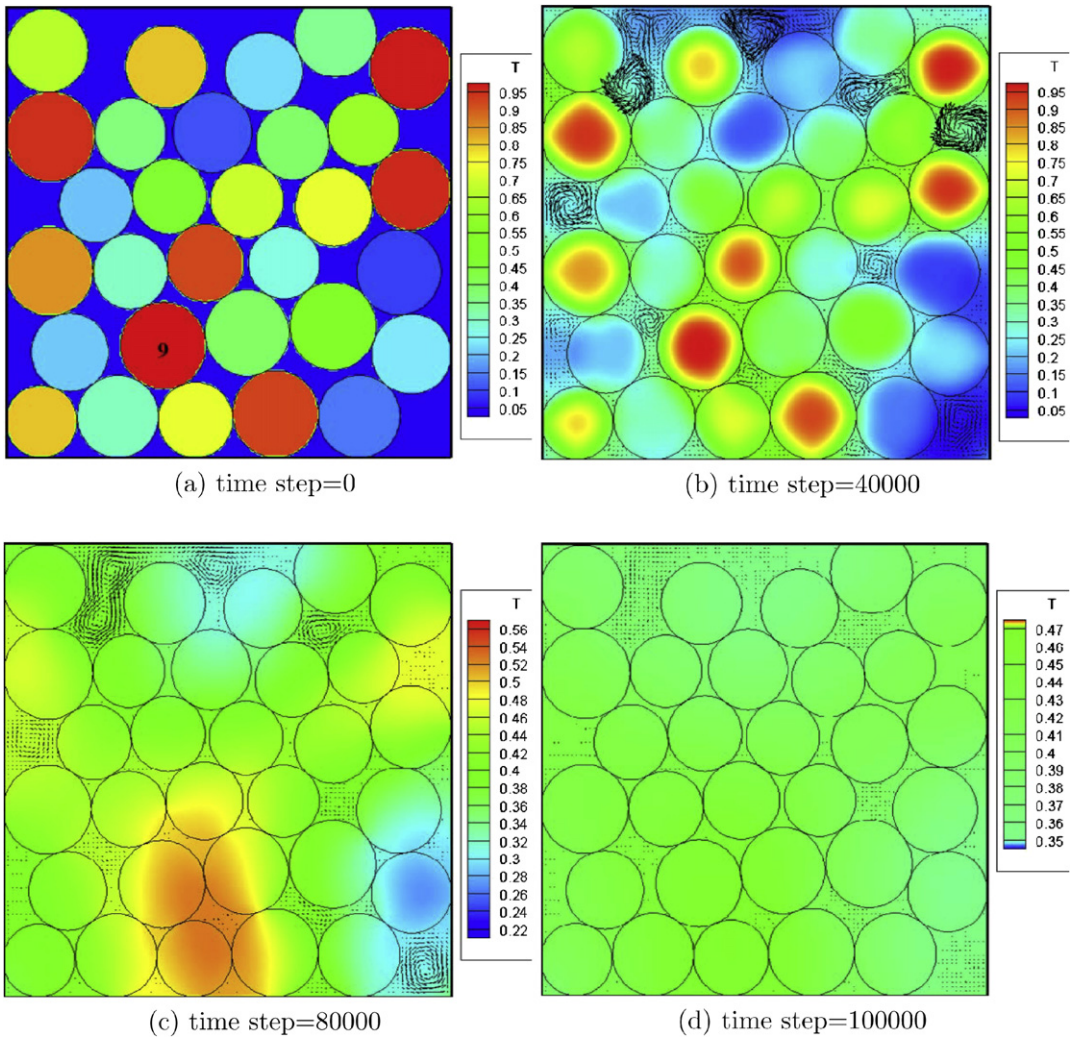

Fig. 7. Heat convection and conduction in a particle system: Temperature distributions at several time instants.

ity $u_{\max}/U^*$ at $y/H = 0.5$, the normalised maximum vertical velocity $v_{\max}/U^*$ at $x/L = 0.5$ and the locations of the maximum velocities.

It can be seen that the results agree very well with each other, indicating that the PPB scheme can indeed be used for treating adiabatic thermal boundary conditions. Fig. 5 illustrates the isothermal contours for different Rayleigh numbers.

The second example simulates heat transfer in a system comprising 30 circular particles that are randomly generated by the advancing-front packing algorithm [18], and are in contact with their neighbouring particles, as shown in Fig. 6(a). The particles have different initial temperatures ranging from 0 to 1, and the four walls are adiabatic. The domain is divided into a 200×200 lattice. The model parameters are chosen as $Ra = 10^5$, $Pr = 0.71$, $\tau_f = 0.05$ and $\tau_g = 0.005$. Two approaches, the PPB scheme proposed in this work and the non-slip thermal boundary approach proposed by Huang et al. [16], are employed for handling the insulated outer boundaries. Fig. 6 plots the temperature evolution histories of particle No. 9 obtained by the two approaches. It is clear that the results have an excellent correspondence. Fig. 7 depicts the temperature contours and total velocity vectors of the particle system at four time instants, from which the complex patterns of thermal and fluid flows, as well as a nearly steady-state thermal equilibrium can be clearly observed.

5. Conclusions

The paper has introduced a novel numerical approach, the partial bounce back scheme, to account for thermal contact resistance between contacting surfaces within the framework of the thermal lattice Boltzmann method. In particular, the correlation between thermal contact resistance R_c and the partial bounce back parameter δ has been established. A special case of the scheme ($\delta = 1$) leads to a new approach which can be directly applied for the treatment of adiabatic thermal boundary conditions in the TLBM. The numerical examples have validated and demonstrated the accuracy and effectiveness of the proposed methodology. Finally, the proposed partial bounce back scheme can be readily extended to the 3D case and the relevant work will be reported elsewhere.

Acknowledgements

This work is partially funded by the EPSRC of UK under grant Nos. GR/R92318/01 and EP/C51520X/1. The support is gratefully acknowledged. The authors would also like to thank Dr. H. Huang, Dr. A. D'Orazio, Prof. G. Tang and Dr. J. Wang for their valuable discussions during the early stage of this work.

References

[1] C.K. Aidun, Y. Lu, E.-G. Ding, Direct analysis of particulate suspensions with inertia using the discrete Boltzmann equation, Journal of Fluid Mechanics 373 (1998) 287–311.
[2] B.K. Cook, D.R. Noble, J.R. Williams, A direct simulation method for particle-fluid systems, Engineering Computations 21 (2–4) (2004) 151–168.
[3] Z.G. Feng, E.E. Michaelides, Proteus: a direct forcing method in the simulations of particulate flows, Journal of Computational Physics 202 (2005) 20–51.
[4] Y.T. Feng, K. Han, D.R.J. Owen, Coupled lattice Boltzmann method and discrete element modeling of particle transport in turbulent fluid flows: Computational issues, International Journal for Numerical Methods in Engineering 72 (2007) 1111–1134.
[5] K. Han, Y.T. Feng, D.R.J. Owen, Coupled lattice Boltzmann and discrete element modelling of fluid–particle interaction problems, Computers and Structures 85 (2007) 1080–1088.
[6] K. Han, Y.T. Feng, D.R.J. Owen, Numerical simulations of irregular particle transport in turbulent flows using coupled LBM-DEM, Computer Modelling in Engineering & Sciences 18 (2) (2007) 87–100.
[7] A. Ladd, R. Verberg, Lattice–Boltzmann simulations of particle–fluid suspensions, Journal of Statistical Physics 104 (5/6) (2001) 1191–1251.
[8] H. Yu, S. Girimaji, L. Luo, DNS and LES of decaying isotropic turbulence with and without frame rotation using lattice Boltzmann method, Journal of Computational Physics 209 (2005) 599–616.
[9] X. He, S. Chen, G.R. Doolen, A novel thermal model for the lattice Boltzmann method in incompressible limit, Journal of Computational Physics 146 (1998) 282–300.
[10] S. Feng, P. Dong, M. Tsutahara, N. Takada, Simulation of shockwave propagation with a thermal lattice Boltzmann model, International Journal for Numerical Methods in Fluids 41 (2003) 1137–1146.
[11] Z. Guo, B. Shi, C. Zheng, A coupled lattice BGK model for the Boussinesq equations, International Journal for Numerical Methods in Fluids 39 (2002) 325–342.
[12] C. Shu, X.D. Niu, Y.T. Chew, A lattice Boltzmann kinetic model for microflow and heat transfer, Journal of Statistical Physics 121 (1/2) (2005) 239–255.
[13] J. Wang, M. Wang, Z. Li, A lattice Boltzmann algorithm for fluid solid conjugate heat transfer, International Journal of Thermal Sciences 46 (2007) 228–234.
[14] A.Z. D'Orazio, M. Corcione, G.P. Celata, Application to natural convection enclosed flows of a lattice Boltzmann BGK model coupled with a general purpose thermal boundary condition, International Journal of Thermal Sciences 43 (2004) 575–586.
[15] G.H. Tang, W.Q. Tao, Y.L. He, Thermal boundary condition for the thermal lattice Boltzmann equation, Physical Review E 72 (2005) 016703.
[16] H. Huang, T.S. Lee, C. Shu, Thermal curved boundary treatment for the thermal lattice Boltzmann equation, International Journal of Modern Physics C 17 (5) (2006) 631–643.
[17] J.P. Hollman, Heat Transfer, McGraw-Hill, 1997.
[18] Y.T. Feng, K. Han, D.R.J. Owen, Filling domains with disks: An advancing front approach, International Journal for Numerical Methods in Engineering 56 (2003) 699–713.